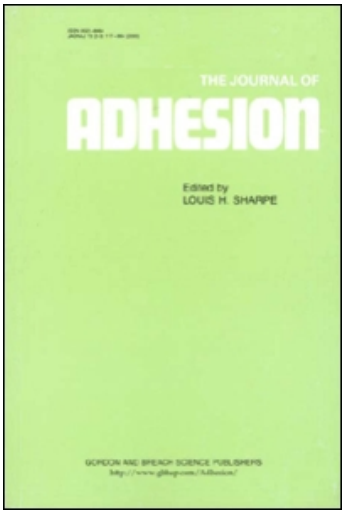

The Journal of Adhesion
Publication details, including instructions for authors and subscription information:
http://www.informaworld.com/smpp/title~content=t713453635

A Model to Predict the Anomalous Fatigue Crack Growth Behaviour Seen in Mixed Mechanism Fracture

I. A. Ashcroft[a]; J. P. Casas-Rodriguez[a]; V. V. Silberschmidt[a]
[a] Wolfson School of Mechanical and Manufacturing Engineering, Loughborough University, Leicestershire, UK

Online publication date: 10 June 2010

To cite this Article Ashcroft, I. A. , Casas-Rodriguez, J. P. and Silberschmidt, V. V.(2010) 'A Model to Predict the Anomalous Fatigue Crack Growth Behaviour Seen in Mixed Mechanism Fracture', The Journal of Adhesion, 86: 5, 522 — 538
To link to this Article: DOI: 10.1080/00218464.2010.484306
URL: http://dx.doi.org/10.1080/00218464.2010.484306

The Journal of Adhesion, 86:522–538, 2010

ISSN: 0021-8464 print/1545-5823 online
DOI: 10.1080/00218464.2010.484306

Taylor & Francis
Taylor & Francis Group

A Model to Predict the Anomalous Fatigue Crack Growth Behaviour Seen in Mixed Mechanism Fracture

I. A. Ashcroft, J. P. Casas-Rodriguez, and V. V. Silberschmidt
Wolfson School of Mechanical and Manufacturing Engineering, Loughborough University, Leicestershire, UK

Adhesive bonding is an attractive joining method for fibre reinforced polymers (FRPs); however, if adhesive joints are to be used in structural applications, methods of accurately predicting mechanical performance are required. In many structural applications the joints will be subjected to cyclical loading, in which case fatigue performance must be considered. One of the most useful methods of analysing fatigue is through the application of fracture mechanics, in which the fatigue crack growth rate is related to an appropriate fracture mechanics parameter, such as strain energy release rate. This relationship is often plotted on a fatigue crack growth (FCG) plot and an empirical FCG law derived by fitting an appropriate form of equation to this plot. However, in bonded composite joints, anomalous FCG is seen when mixed mode samples are tested. In this paper, this anomalous behaviour is explained and a mechanistically based model for predicting this behaviour is proposed. The model is applied to experimental data and a good fit is seen.

Keywords: Anomalous crack growth; CFRP; Epoxy; Fatigue; Fracture mechanics; Mixed mechanism fracture

1. INTRODUCTION

Carbon fibre reinforced polymer composites (CFRPs) are used in many high-performance applications, such as aircraft, high speed marine vessels, racing cars, and high technology sports equipment. An obvious reason for using these materials is the high specific

Received 7 February 2010; in final form 22 March 2010.
Presented in part at the 3rd International Conference on Advanced Computational Engineering and Experimenting (ACE-X 2009), Rome, Italy, 22–23 June 2009.
Address correspondence to I. A. Ashcroft, Wolfson School of Mechanical and Manufacturing Engineering, Loughborough University, Leicestershire LE11 3TU, UK. E-mail: i.a.ashcroft@iboro.ac.uk

strength and stiffness; however, other potential advantages include reparability, insulating properties, corrosion resistance, use in stealth applications, and fatigue resistance. The two main methods for joining CFRPs are mechanical joining, mainly riveting and bolting, and adhesive bonding. Mechanical bonding is usually preferred for thicker sections, in which peel stresses are high in bonded joints, and where disassembly is required. However, for thinner sections, adhesive bonding has a number of advantages, including increased stiffness, reduced weight, sealing ability, and the removal of the requirement to drill a hole in the CFRP. However, certain disadvantages are also associated with adhesive bonding. These include sensitivity to the manufacturing process (particularly, poor surface preparation), difficulty in detecting poorly bonded areas, environmental sensitivity, and a lack of analysis methods for real, in-service conditions. Most of these problems can be overcome and there has been significant work done in the adhesive bonding of composite parts [1–5].

One of the main concerns in designing any load-bearing structure is resistance to fatigue and it has been estimated that 80% of engineering failures involve fatigue [6]. The reduction in damage to the composite and increase in stiffness of bonded joints compared with mechanically fastened joints would indicate improved fatigue resistance, and research has shown that good fatigue resistance can, indeed, be seen in bonded composite joints [7–9]. However, it has also been seen that fatigue failure in bonded composite joints can involve complex, mixed mechanism failures [10–14].

One of the most useful methods of analysing fatigue in structures is through the fracture mechanics, or fatigue crack growth (FCG), approach. In this method, the fatigue crack growth rate (da/dN) is related to an appropriate fracture mechanics parameter. This is usually the strain energy release rate (G) or the J-integral (J) in the case of adhesively bonded joints [15–25]. A typical plot of log ΔG against log da/dN is shown in Fig. 1a, where ΔG is the strain energy release rate amplitude. It can be seen that the FCG curve has a characteristic sigmoidal shape. Region I of this curve is associated with a fatigue threshold (ΔG_{th}), below which measurable crack growth does not occur. In Region II, the FCG curve is essentially linear and in many cases a Paris-type relationship [26], as given below, fits this region of the data well.

$$\frac{\mathrm{da}}{\mathrm{dN}} = \mathrm{C}(\Delta \mathrm{G})^{m}, \tag{1}$$

where C and m can, within certain constraints, be considered material constants. Region III of the FCG curve signifies unstable crack growth

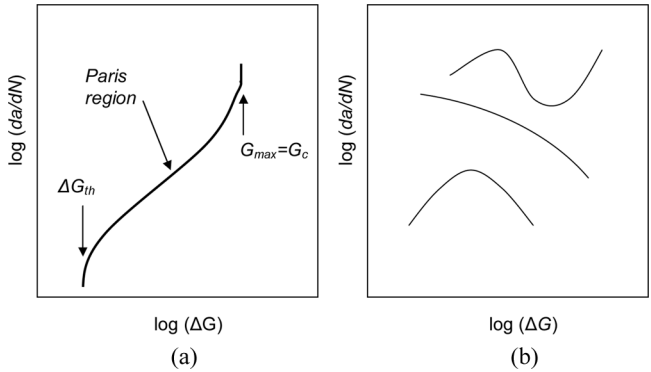

FIGURE 1 Fatigue crack growth (FCG) plots showing (a) standard behaviour and (b) examples of anomalous behaviour.

as the upper value of G in the fatigue spectrum, G_{max}, approaches the critical strain energy release rate in quasi-static loading, G_c. The Paris curve together with ΔG_{th} and G_c can be used as a simple representation of the complete FCG curve. Alternatively, a more complex equation can be used to represent the full curve, an example of which is shown below [27].

$$\frac{da}{dN} = C(G_{max})^m \left\{ \frac{1 - \left(\frac{G_{th}}{G_{max}}\right)^{m_1}}{1 - \left(\frac{G_{max}}{G_c}\right)^{m_2}} \right\}, \tag{2}$$

where m_1 and m_2 are additional material constants.

However, in some cases, particularly when testing mixed mode bonded composite joints, anomalous FCG plots are seen. These are those shown schematically in Fig. 1b and demonstrate such features as reverse slope Paris regions and both single and double turning points. This paper will provide an experimental example of anomalous FCG and provide an explanation for this type of behaviour. A mechanistically based method of predicting this behaviour is then proposed and applied to the experimental data presented in the paper.

2. EXPERIMENTAL

2.1. Experimental Materials

The adhesively bonded joints used in the experimental work consisted of CFRP adherends joined with an aerospace-grade toughened epoxy

TABLE 1 Properties of T800/5245C Composite at Room Temperature

	E_x (GPa)	E_y (GPa)	G_{xy} (GPa)	v_{xy}	v_{yx}
UD	174	9.64	7	0.36	0.02
MD	99.8	28.1	25.7	0.69	0.2

film adhesive. The CFRP used was Rigidite® 5245C matrix with 0.6 volume fraction of unidirectional T800 fibres. This was supplied by Cytec Engineered Materials Ltd., Wrexham, U.K., in the form of nominally 0.125-mm thick pre-preg. A multidirectional (MD) lay-up scheme of $[(0/-45/+45/0)_2]_S$ was used to manufacture panels 2-mm thick. These were cured for 2 hours at 182°C with an initial autoclave pressure of approximately 600 kN/m^2. The elastic properties of the cured CFRP are given in Table 1. The unidirectional (UD) properties are from experimental testing at the Defence Research Agency (DRA), Farnborough, UK and the MD properties are then determined by laminate analysis. The adhesive used was EA9628 from Hysol Dexter, Windsor Locks, OT, U.S.A. (now part of the Loctite Corp., Dusseldorf, Germany), which is a rubber-toughened single-part epoxy film adhesive of 0.2-mm nominal thickness. The true stress-strain behaviour of the adhesive from tensile testing bulk dumbbell samples can be seen in Fig. 2. True stress was determined assuming a Poisson's ratio of 0.5 in the plastic region.

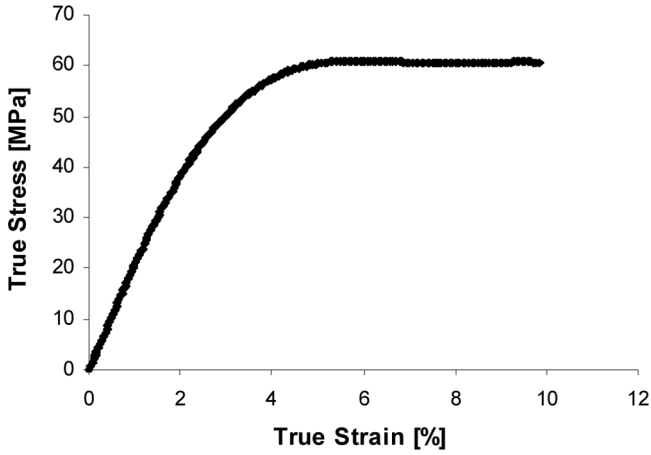

FIGURE 2 Stress-strain curve for adhesive EA9628.

2.2. Sample Preparation

In this study the bonded joints used in the experimental programme were lap-strap joints. These are long overlap joints and demonstrate behaviour more representative of many of those seen in real aerospace applications, such as the bonding of stringers, than the more commonly used short overlap joints, such as the standard single-lap joint. Lap-strap joints, of the dimensions shown in Fig. 3, were manufactured for the fatigue testing. Cured CFRP panels were grit blasted and acetone cleaned prior to bonding. The adhesive was cut to size and placed between the prepared CFRP panels and the assembly cured under pressure in an autoclave for 60 min at 120°C. Fatigue samples were cut from the bonded panels using a diamond saw and end tabs were bonded to the samples to aid grip and provide alignment.

2.3. Fatigue Testing

A servo-hydraulic fatigue testing machine with digital control and computer data acquisition was used for the fatigue testing. Load control was used with a maximum load of 7.8 kN, which was approximately 60% of the quasi-static failure load. The waveform was sinusoidal with an R-ratio (minimum-to-maximum load) of 0.1 and frequency of 5 Hz. All testing was in ambient laboratory environmental conditions where temperature and relative humidity varied

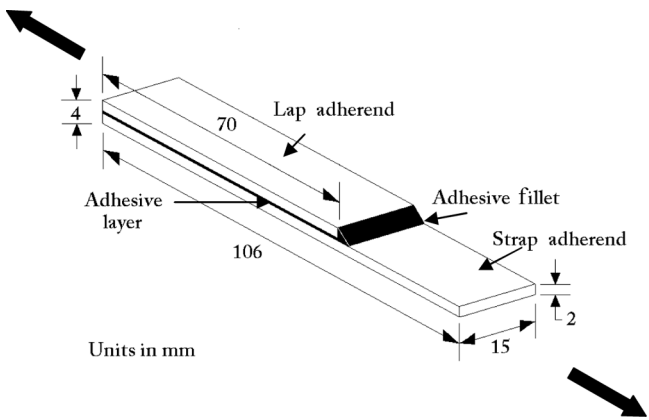

FIGURE 3 Dimensions of lap-strap joint.

between 18–25°C and 50–60%, respectively. Thermocouples were placed at various points on the surfaces of the samples in order to investigate any thermo-elastic heating during testing; however, no change in temperature was observed.

In-situ crack growth was measured both optically and using a resistance-based crack measurement system. The edges of one side of the samples were painted white and marked with a scale prior to testing in order to increase the contrast between cracked and uncracked material. This side was monitored by taking images with a high magnification digital camera at defined intervals. A "Krak Gage" was bonded to the other side, which is the name of the electrical resistance crack gauge manufactured by Rumul A.G., Neuhansen am Rheinfall, Switzerland [28]. This gauge is designed to tear as the crack grows, with the subsequent change in electrical resistivity providing an accurate measure of crack length. The electrical resistance is monitored using Rumul's "Fractomat" and the signal fed into the test machines' computer data acquisition system. After fatigue testing the fracture surfaces were examined using a range of optical and scanning electron microscopes.

3. DETERMINATION OF STRAIN ENERGY RELEASE RATE AND CRACK GROWTH RATE

The first method used to determine the strain energy release rate in the lap-strap joints was a simple analytical method proposed by Brussat and Chiu [29]. For the rest of this paper it will be referred to as the Brussat model. This model is based on an elastic analysis of an infinite beam in which the adhesive layer is neglected. The total strain energy release rate (G_T) is defined as the sum of the Mode I and Mode II contributions (*i.e.*, $G_T = G_I + G_{II}$) and for the Brussat model G_T is termed G_{Brus}.

$$G_{Brus} = \frac{P^2}{2b_N(EA)_2}\left[1 - \frac{(EA)_2}{(EA)_0}\right], \tag{3}$$

where P is the load, b_N is specimen width, $(EA)_2$ is the tensile rigidity of the strap, and $(EA)_0$ is the total rigidity (lap + strap). Analyzing Eq. (3), it can be seen that G_{Brus} is independent of the crack size. It was further shown in [29] that the ratio between G_I/G_T for equal thickness adherends using this model is 4/7.

Strain energy release rate was also determined from a geometric non-linear finite element analysis (FEA) using the virtual crack closure technique [30]. The lap-strap joint was modelled using the commercial FEA software package MARC-MENTAT (2007-R1) from MSC Software Corp., Santa Ana, CA, U.S.A. Four-noded plane strain isoparametric elements with assumed strain interpolation were used as these gave the best compromise between accuracy in the calculation of fracture mechanics parameters and computational efficiency. However, this meant that a high degree of mesh refinement was necessary to remove any mesh dependency in the fracture mechanics parameters determined from the FEA models. Both materials were modelled as linear elastic, with the composite having the properties shown in Table 1 and adhesive having elastic modulus and Poisson's ratio of 2.24 GPa and 0.38, respectively. The boundary conditions used in the model are shown in Fig. 4a and the mesh in the overlap region prior to the introduction of a crack can be seen in Fig. 4b.

Three locations of cracking were explored in the models, corresponding to the locations of fracture seen in the experimental testing. Figure 5a shows a crack in the centre of the adhesive layer, Fig. 5b shows a crack at the interface between the CFRP strap adherend and the adhesive layer, and Fig. 5c shows a crack in the first ply of the strap adherend, adjacent to the adhesive layer. The variation in G_T with crack length for these three crack locations, together with the result from Eq. (3), are plotted in Fig. 6. It can be seen that the three FEA results are similar, indicating that crack location does not have a significant effect on the calculated strain energy release rate. The resistance to crack growth, of course, may be significantly different in the different locations. For small crack sizes the FEA results agree quite well with the results from Eq. (3); however,

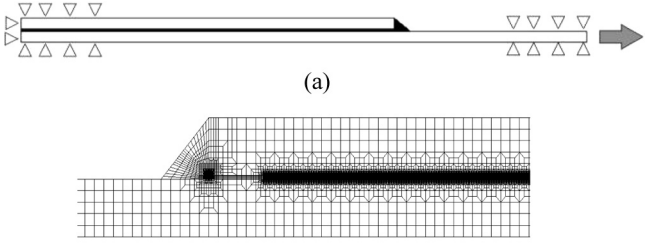

FIGURE 4 Finite element model. (a) Boundary conditions. (b) Mesh in the overlap area prior to cracking.

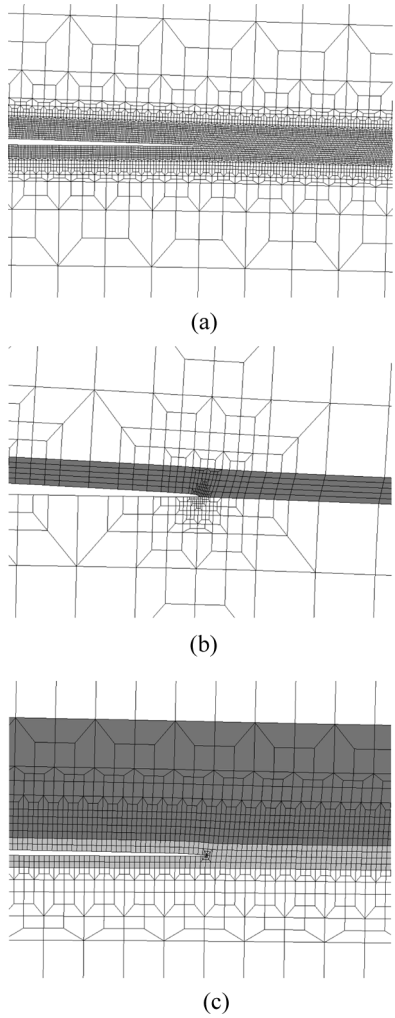

FIGURE 5 Finite element meshes for (a) fracture in the adhesive, (b) interfacial fracture, (c) fracture in first ply of the composite.

at longer crack lengths the strain energy release rate decreases in the FEA models but remains constant in Brussat's model. This highlights the inability of the analytical model to account for edge effects and geometric non-linearity. In the rest of this work strain energy release rate is determined using the non-linear FEA with appropriate crack location.

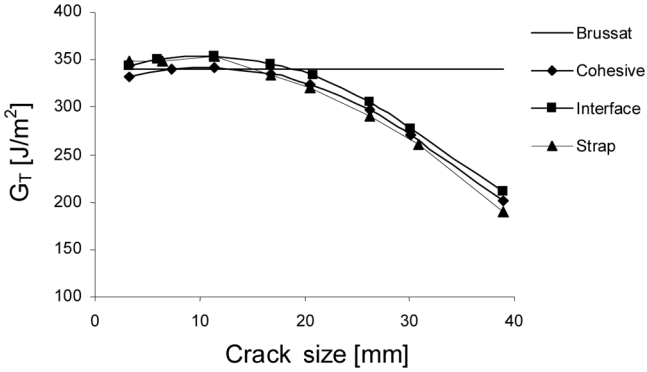

FIGURE 6 Comparison of strain energy release rate (G) determined using an analytical model (Brussat) and FEA with different fracture paths.

4. RESULTS

Fatigue testing of the bonded CFRP joints resulted in two types of failure, as illustrated schematically in Fig. 7. Note that crack path and fillet shape and size are illustrative in these figures, being simplified and omitting the variations seen in the actual test samples. In the first type of failure, shown in Fig. 7a, the fatigue crack initiated in the fillet area of the adhesive and then continued to propagate through the adhesive layer. In the second type of failure, the fatigue

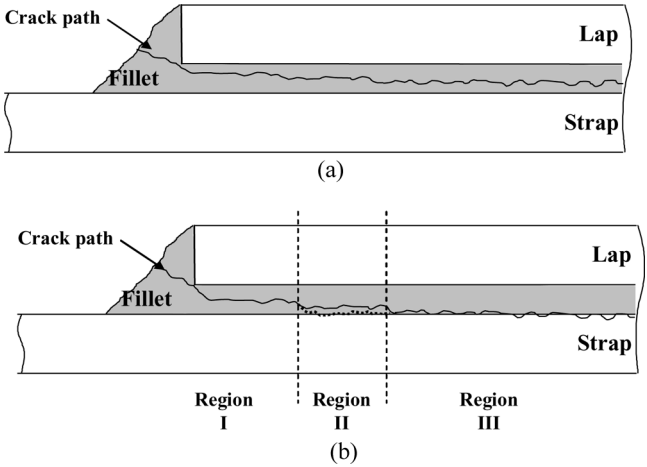

FIGURE 7 Crack path schematic, showing: (a) cohesive fracture in adhesive and (b) a mixed-mechanism fracture path.

crack initiated in the adhesive, as before, and progressed for a while in the adhesive layer. This is labelled Region I in Fig. 7b. However, the crack then progressed to the interfacial region between the adhesive layer and the first ply of the CFRP in the strap adherend. In this region a mix of failure in the adhesive and in the matrix of the 0° degree ply of the strap adherend adjacent to the adhesive is observed. This is named Region II in Fig. 7b and can also be seen in the optical photograph of a fracture surface in Fig. 8. Eventually the fatigue crack progresses entirely in the CFRP. This is labelled Region III in Figs. 7b and 8.

Typical plots of fatigue crack growth (FCG) rate against crack length for samples exhibiting the two types of crack growth discussed above can be seen in Fig. 9. The sample in which fracture was entirely within the adhesive layer exhibits a decreasing FCG rate with crack length, consistent with the decreasing value of G with crack length shown in Fig. 6. The sample showing mixed mechanism fracture follows the plot for the sample with fracture in the adhesive layer up to approximately 15-mm crack length. This is not surprising, as up until this point the fracture is by the same mechanism in both samples. However, after this point the FCG rate begins to increase for the mixed mechanism fracture sample, even though G is still decreasing. This discontinuity in the FCG rate is coincident with a change in the fracture path from the adhesive layer to a mixed fracture in the adhesive and the CFRP. The increased FCG rate indicates that the fatigue resistance of the CFRP is lower than that of the adhesive. The effect of this on the FCG plot can be seen in Fig. 10. The sample with failure in the adhesive layer shows the standard Paris-type relationship, with the logarithm of FCG rate decreasing linearly with the logarithm of strain energy release rate amplitude, ΔG. At high ΔG, the sample with a mixed mechanism fracture has a similar FCG rate to the sample fracturing in the adhesive. However, after a while there

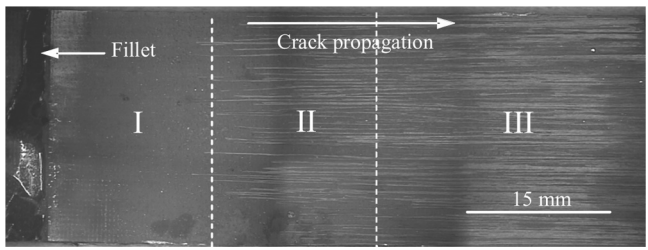

FIGURE 8 Optical image of the fracture surface of a CFRP-epoxy lap-strap joint showing a mixed-mechanism fracture.

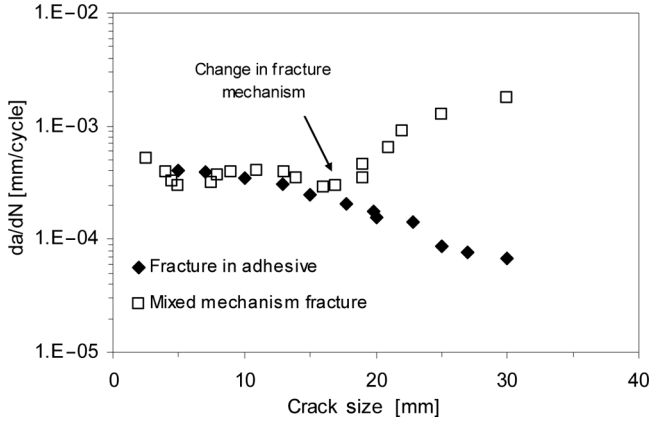

FIGURE 9 Fatigue crack growth rate as a function of crack length for fracture in the adhesive and a mixed-mechanism fracture.

is an increase in the FCG rate with decreasing G. This is an example of the anomalous crack growth behaviour illustrated in Fig. 1b. Obviously, this transition from standard Paris-type behaviour to anomalous behaviour is a result of the change from fracture in the adhesive to the mixed mechanism fracture discussed previously. The FCG plot from testing a CFRP sample with no adhesive layer is also shown in the figure and it can be seen that the FCG plot for the

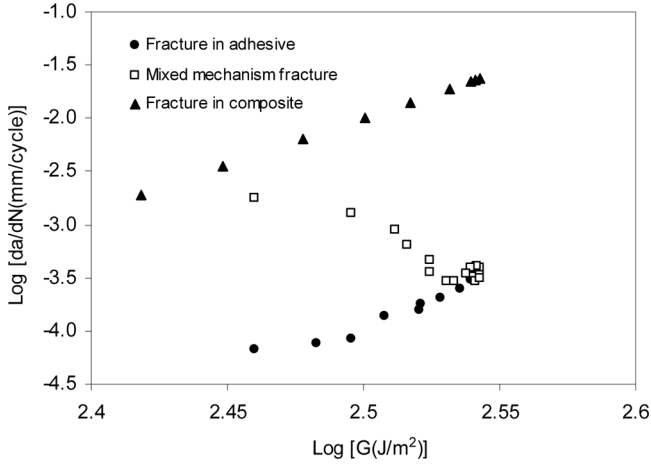

FIGURE 10 Fatigue crack growth plots for fracture in the adhesive layer, in the composite, and a mixed-mechanism fracture.

mixed mechanism sample is tending towards this plot as fracture progresses. It is obvious that the resultant FCG plot for a mixed mechanism fracture is highly dependent on the FCG plots for the various mechanism individually and the proportion of each fracture mechanism. In the next section a method of predicting this behaviour is proposed.

5. MIXED MECHANISM FRACTURE MODEL

It is proposed in the previous section that the FCG rate under mixed mechanism fracture is a function of the FCG rates for the various modes of fracture seen in the mixed mechanism fracture region and the area fractions of the various fracture mechanisms. In the case of a two-mechanism fracture involving fracture in either the composite or the adhesive, as in this case, this can be expressed by:

$$\left(\frac{da}{dn}\right)_m = f\left[A_a, \left(\frac{da}{dn}\right)_a, A_c\left(\frac{da}{dn}\right)_c\right],$$

where A indicates area fraction of failure mode, as seen in the fracture surface, and the subscripts *m, a*, and *c* represent mixed, adhesive, and composite, respectively. The simplest form of this law is a simple additive one, *i.e.*:

$$\left(\frac{da}{dn}\right)_m = A_a\left(\frac{da}{dn}\right)_a + A_c\left(\frac{da}{dn}\right)_c \tag{4}$$

$$\log\left(\frac{da}{dn}\right)_m = \log\left[A_a\left(\frac{da}{dn}\right)_a + A_c\left(\frac{da}{dn}\right)_c\right]. \tag{5}$$

There is a schematic illustration of this model in Fig. 11 for a presumed variation in fractional area of adhesive failure, which is indicated on the plot. It can be seen from this figure that all the anomalous features shown in Fig. 1b, can be predicted by Eq. (4). At high levels of G the fracture is in the adhesive layer and, hence, the FCG rate (da/dn) decreases with decreasing G, following the curve for failure in the adhesive. However, as G continues to decrease, a point is reached where the fracture becomes mixed and the area of adhesive fracture decreases. At this point the mixed mechanism FCG plot shows an increase in FCG rate with decreasing G. As composite fracture begins to dominate, the mixed mechanism FCG plot shows another turning point before becoming coincident with the composite fracture plot at low values of G.

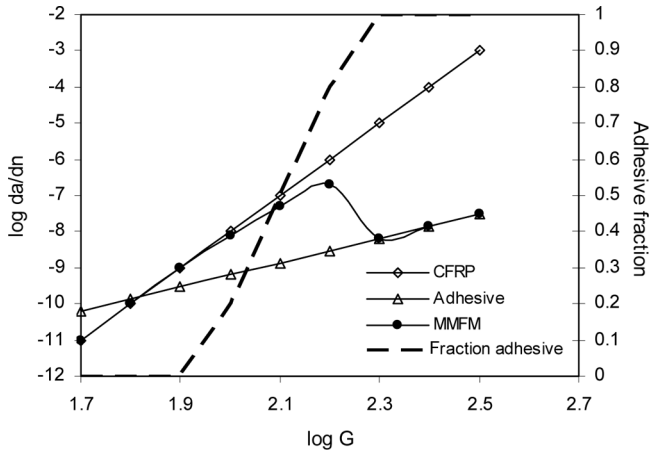

FIGURE 11 Schematic illustration of the proposed mixed-mechanism fatigue fracture model.

Equation (4) assumes there is a proportional relationship between the area fraction of a particular failure mode and its effect on the mixed FCG rate; however, this isn't necessarily the case. It may be the case that one of the fracture mechanisms has a disproportionate effect on the mixed FCG rate. The easiest way to accommodate this is to substitute the actual area fractions, A_i, in Eqs. (4) and (5) with effective area fraction A_i', as illustrated in Eqs. (6) and (7):

$$\left(\frac{da}{dn}\right)_m = A_a'\left(\frac{da}{dn}\right)_a + A_c'\left(\frac{da}{dn}\right)_c \tag{6}$$

$$\log\left(\frac{da}{dn}\right)_m = \log\left[A_a'\left(\frac{da}{dn}\right)_a + A_c'\left(\frac{da}{dn}\right)_c\right]. \tag{7}$$

A method of mapping the actual area fraction to the effective area fraction is required and two possible methods are illustrated in Fig. 12. Figure 12a shows the mapping of composite failure fraction, A_c, to an effective composite area fraction, A_c', through the use of power laws. It can be seen that by selecting the order of the power, the nature and extent of the mapping between the measured and effective fractional areas can be controlled. An alternative is to use polynomial functions, as shown in Fig. 12b. In this figure it can be seen how a second order polynomial can be used to devise a mapping function in which the fracture is dominated by whichever mechanism has the greater area fraction.

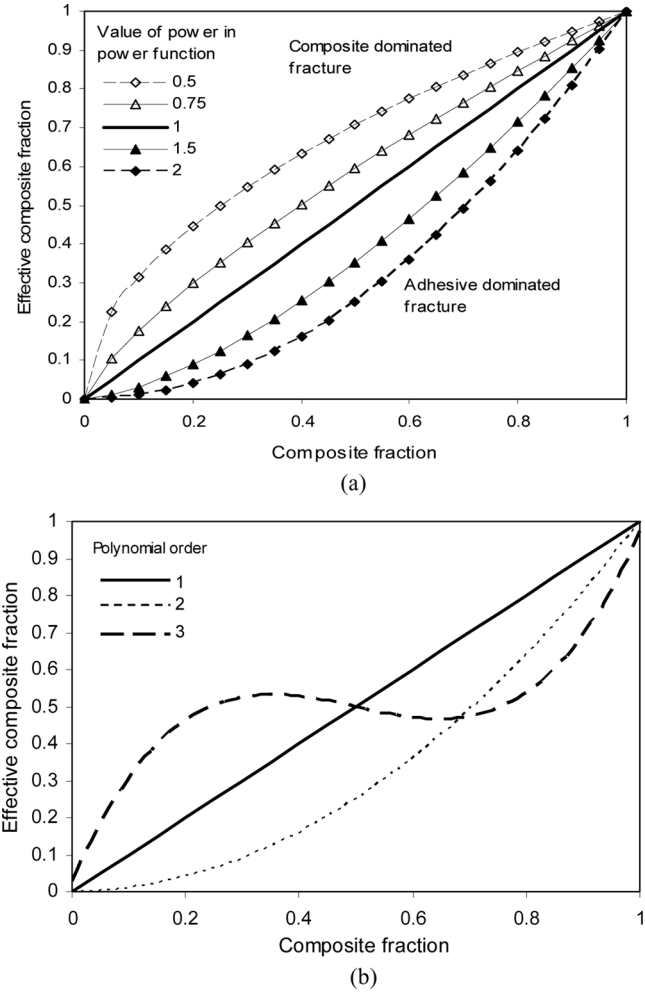

FIGURE 12 Determination of effective composite fraction using (a) power law functions and (b) polynomial functions.

The proposed mixed-mechanism fatigue fracture model (MMFM) was applied to the experimental results presented in Section 4 of the paper. The first step was to determine the area fractions of each mechanism. This was achieved by importing a digital photograph of the fracture surface into an image analysis software package. The image was converted to a grey scale and the contrast between the different failure modes enhanced. The grey scale image was then converted into a two bit (*i.e.*, black and white) image using the mathematical software

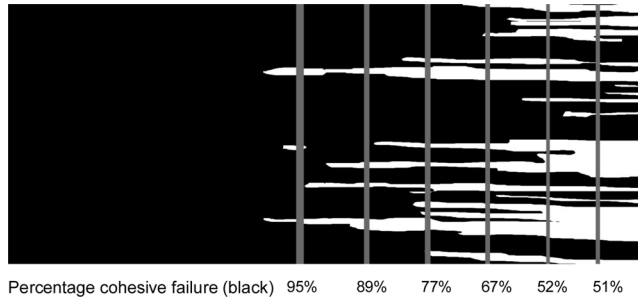

FIGURE 13 Digitised image of fracture surface showing fracture in the adhesive in black and fracture in the composite in white.

Matlab from The Mathworks, Natiak, MA, Ltd., USA. A Matlab pixel counting subroutine was then used to calculate the percentage of each fracture mode. This process is illustrated in Fig. 13, which shows the two bit fracture surface image and the determination of area fraction as a function of crack length. The next step was to determine a suitable mapping function in order to determine the effective fractional areas. In this case this was done by trial and error; however, with more data a more effective method of optimising the parameters in the mapping function could be used. The results of applying Eq. (6) to the experimental data are shown in Fig. 14. It can be seen that

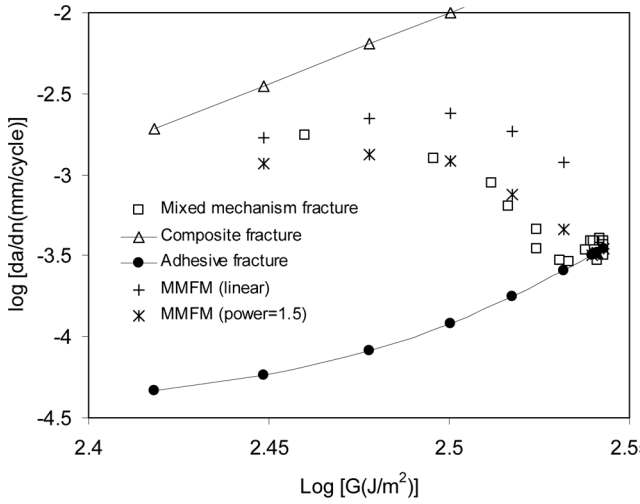

FIGURE 14 Application of the mixed-mechanism fracture model (MMFM) to experimental data using linear and power law mapping between measured and effective fractional areas.

the MMFM with a linear relationship between actual and effective fractional area tends to overestimate the effect of the composite fracture at low fractions of composite failure, resulting in an over-prediction of the FCG rate. This was improved by using a power law of 1.5 in the mapping relationship, which created an adhesive facture domination at high area fractions of adhesive fracture. It can be seen in Fig. 14 that this results in a good prediction of the experimental mixed-mechanism FCG plot.

6. SUMMARY AND CONCLUSIONS

This paper has shown evidence of anomalous fatigue crack growth plots in bonded composite joints. This behaviour has been attributed to the nature of the fatigue fracture, in which a complex fracture path was observed involving failure in both the adhesive layer and the composite adherend. A simple model, based on the FCG plots for the individual fracture mechanisms and the area fractions of each fracture mechanism, was proposed. It was noted that a proportional relationship between the measured area fraction and its influence on the mixed-mechanism fracture cannot be assumed and hence a method of mapping the measured area fraction to an effective area fraction was also proposed. The model described above was shown to be able to predict all the observed anomalous fatigue crack growth behaviour and could quantifiably predict experimental results to a good degree of accuracy. Although this method has only been demonstrated for the case of bonded composite joints, in which fracture in the adhesive and CFRP was observed, it is envisaged that a similar method could be applied to any fatigue fracture incorporating mixed-mechanism failure.

REFERENCES

[1] Davies, P., *Adhesive bonding: Science, Technology and Applications*, (Woodhead Publishing, Cambridge, 2005), Ch. 13, pp. 279–301.
[2] Tong, L. and Steven, G. P., *Analysis and Design of Structural Bonded Joints*, (Kluwer Academic Publishing, London, 1999).
[3] Adams, R. D., Comyn, J., and Wake, W. C., *Structural Adhesive Joints in Engineering*, 2nd ed. (Chapman and Hall, London, 1997).
[4] Hart-Smith, L. J., *J. Comp. Tech. Res.* **24**, 133–153 (2002).
[5] Ashcroft, I. A., Hughes, D. J., and Shaw, S. J., *Assembly Autom.* **20**, 150–161 (2000).
[6] Dowling, N. E., *Mechanical Behaviour of Materials: Engineering Methods for Deformation, Fracture and Fatigue*, (Prentice Hall, Upper Saddle River, 1998).
[7] Schön, J. and Starikov, R., *Fatigue in composites*, (Woodhead Publishing, Cambridge, 2000), Ch. 23, pp. 621–643.
[8] Mall, S., Ramamurthy, G., and Rezaizdeh, M. A., *Compos. Struct.* **8**, 31–45 (1987).

[9] Ashcroft, I. A., Abdel Wahab, M. M., Crocombe, A. D., Hughes, D. J., and Shaw, S. J., *J. Adhesion* **75**, 61–88 (2001).
[10] Ashcroft, I. A., Abdel Wahab, M. M., Crocombe, A. D., Hughes, D. J., and Shaw, S. J., *Compos. Part A-Appl. Sci.* **32**, 45–58 (2001).
[11] Erpolat, S., Ashcroft, I. A., Crocombe, A. D., and Abdel-Wahab, M. M., *Int. J. Fatigue* **26**, 1189–1196 (2004).
[12] Ashcroft, I. A., *J. Strain Anal. Eng.* **39**, 707–716 (2004).
[13] Casas-Rodriguez, J. P., Ashcroft, I. A., and Silberschmidt, V. V., *Comp. Sci. Technol.* **68**, 2663–2670 (2008).
[14] Ashcroft, I. A., Casas-Rodriguez, J. P., and Silberschmidt, V. V., *J. Mat. Sci.* **43**, 6704–6713 (2008).
[15] Mostovoy, S., Crosley, P. B., and Ripling, E. J., *J. Materials* **2**, 661–681 (1967).
[16] Kinloch, A. J. and Shaw, S. J., *J. Adhesion* **12**, 59–77 (1981).
[17] Mall, S. and Johnson, W. S., *Characterization of Mode I and Mixed-Mode Failure of Adhesive Bonds Between Composite Adherends*, NASA Technical Memorandum 86355, (NASA, Hampton, 1985).
[18] Fernlund, G. and Spelt, J. K., *Int. J. Adhes. Adhes.* **11**, 213–220 (1991).
[19] Lin, C. and Liechti, K. M., *J. Adhesion* **21**, 1–24 (1987).
[20] Ashcroft, I. A., Hughes, D. J., and Shaw, S. J., *Int. J. Adhes. Adhes.* **21**, 87–99 (2001).
[21] Erpolat, S., Ashcroft, I. A., Crocombe, A., and Abdel Wahab, M., *Eng. Fract. Mech.* **71**, 1393–1401 (2004).
[22] Hadavinia, H., Kinloch, A. J., Little, M. S. G., and Taylor, A. C., *Int. J. Adhes. Adhes.* **23**, 463–471 (2003).
[23] Abdel Wahab, M. M., Ashcroft, I. A., Crocombe, A. D., Hughes, D. J., and Shaw, S. J., *Compos. Part A-Appl. Sci.* **32**, 59–69 (2001).
[24] Fernlund, G. and Spelt, J. K., *Eng. Fract. Mech.* **40**, 119–132 (1991).
[25] Ashcroft, I. A., Abdel-Wahab, M. M., and Crocombe, A. D., *Mech. Adv. Mater. Struct.* **10**, 227–248 (2003).
[26] Paris, P. C. and Erdogan, F., *T. ASME D* **85**, 528–535 (1963).
[27] Ewalds, H. L., *Fracture Mechanics*, (Edward Arnold, London, 1984).
[28] Pankevicius, E. R. and Spicer, M., *J. Mater. Sci.* **25**, 3079–3082 (1990).
[29] Brussat, T. R. and Chiu, S. T., *Fracture Mechanics for Structural Adhesive Bonds – Final Report*, AFML Technical Report, TR-77-163, (Air Force Materials Laboratory, 1977).
[30] Sethuraman, R. and Maiti, S. K., *Eng. Fract. Mech.* **30**, 227–231 (1988).